

Delayed Puberty but Normal Fertility in Mice With Selective Deletion of Insulin Receptors From *Kiss1* Cells

Xiaoliang Qiu, Abigail R. Dowling, Joseph S. Marino, Latrice D. Faulkner, Benjamin Bryant, Jens C. Brüning, Carol F. Elias, and Jennifer W. Hill

Center for Diabetes and Endocrine Research (X.Q., A.R.D., J.S.M., L.D.F., J.W.H.), Department of Physiology and Pharmacology, and Department of Obstetrics-Gynecology (J.W.H.), University of Toledo College of Medicine, Toledo, Ohio 43614; Chemistry Department (B.B.), Carnegie Mellon University, Pittsburgh, Pennsylvania 15213; Institute for Genetics (J.C.B.), Department of Mouse Genetics and Metabolism, Cologne Excellence Cluster for Cellular Stress Responses in Aging Associated Diseases, and Center for Molecular Medicine Cologne, Second Department for Internal Medicine, University of Cologne, and Max Planck Institute for the Biology of Aging, D-50674 Cologne, Germany; and Department of Molecular and Integrative Physiology (C.F.E.), University of Michigan, Ann Arbor, Michigan 48109

Pubertal onset only occurs in a favorable, anabolic hormonal environment. The neuropeptide kisspeptin, encoded by the *Kiss1* gene, modifies GnRH neuronal activity to initiate puberty and maintain fertility, but the factors that regulate *Kiss1* neurons and permit pubertal maturation remain to be clarified. The anabolic factor insulin may signal nutritional status to these neurons. To determine whether insulin sensing plays an important role in *Kiss1* neuron function, we generated mice lacking insulin receptors in *Kiss1* neurons ($IR^{\Delta K_{iss}}$ mice). $IR^{\Delta K_{iss}}$ females showed a delay in vaginal opening and in first estrus, whereas $IR^{\Delta K_{iss}}$ males also exhibited late sexual maturation. Correspondingly, LH levels in $IR^{\Delta K_{iss}}$ mice were reduced in early puberty in both sexes. Adult reproductive capacity, body weight, fat composition, food intake, and glucose regulation were comparable between the 2 groups. These data suggest that impaired insulin sensing by *Kiss1* neurons delays the initiation of puberty but does not affect adult fertility. These studies provide insight into the mechanisms regulating pubertal timing in anabolic states. (***Endocrinology* 154: 1337–1348, 2013**)

The onset of puberty occurs when GnRH neurons are released from the suppression of the prepubertal period (1). Although much of the variance in timing of pubertal onset in humans is due to genetic factors, an estimated 20% to 50% of the variance is due to environmental and metabolic factors that modulate the reemergence of GnRH pulses (1). Reproduction is a metabolically demanding function that requires sufficient levels of energy stores (2). In humans and rodents, insufficient caloric intake or excessive energy expenditure can delay the pubertal transition (3, 4). In addition, disease states associated with metabolic disturbances, including malnu-

trition, chronic inflammatory states, thyroid disease, and GH deficiency, are also associated with a disruption in the normal timing of puberty (5), suggesting that GnRH activation at puberty requires a positive energy balance.

Accordingly, a sophisticated network of regulatory signals linking metabolism and reproduction has evolved to ensure appropriate regulation of GnRH secretion. One such metabolic signal is the pancreatic hormone insulin. Insulin levels circulate in proportion to adipose tissue stores in most mammals (6). Insulin receptors (IRs) and insulin signaling proteins are widely distributed throughout the hypothalamus (7). Hypothalamic insulin signaling

ISSN Print 0013-7227 ISSN Online 1945-7170

Printed in U.S.A.

Copyright © 2013 by The Endocrine Society

doi: 10.1210/en.2012-2056 Received October 17, 2012. Accepted January 16, 2013.

First Published Online February 7, 2013

Abbreviations: ARC, arcuate nucleus; AVPV, anteroventral periventricular nucleus; CV, coefficient of variance; EB, estradiol benzoate; FACS, fluorescence-activated cell sorting; GFP, green fluorescent protein; GTT, glucose tolerance test; HPG, hypothalamic-pituitary-gonadal; IR, insulin receptor; ITT, insulin tolerance test; OVX, ovariectomy; PND, postnatal day.

plays a pivotal role in the regulation of reproduction. Indeed, insulin has been shown to activate GnRH and LH secretion in vitro (8, 9). Mice that lack insulin signaling in brain neurons (NIRKO mice) exhibit hypothalamic hypogonadism (10) and a delay in puberty (11). Moreover, diabetic rats display reproductive abnormalities, which can be ameliorated by central administration of insulin (12–14). In humans, type 1 diabetes also disrupts puberty and reproduction (15, 16).

Although insulin was originally thought to be acting directly on GnRH neurons (8, 9, 17, 18), a recent study suggested otherwise. Deletion of the receptor for a related growth factor, IGF-1, from GnRH neurons resulted in a 3-day delay in pubertal onset, but deletion of the insulin receptor itself from these neurons had no effect on pubertal timing or adult fertility (19). Together, these studies suggest that insulin signaling in presynaptic neurons is important for normal GnRH neuronal function.

Kisspeptin (a product of the *Kiss1* gene) is a key hypothalamic neuropeptide involved in initiating puberty and maintaining reproductive function (20). The hypothalamic *Kiss1* system undergoes a complex pattern of neuroanatomical maturation and functional activation during the course of puberty. Hypothalamic *Kiss1* expression increases during puberty (20, 21), as does the number of anteroventral periventricular nucleus (AVPV) *Kiss1* neurons (particularly in the female) and their putative contacts with GnRH neurons (22). Pubertal maturation does not occur in humans and mice with inactivating mutations in the *Kiss1* gene or the kisspeptin receptor (23–27). Furthermore, kisspeptin administration accelerates the normal progression of puberty in rats, whereas pharmacological blockade of kisspeptin activity disrupts it (28, 29).

Kiss1 neurons have been hypothesized to serve as the primary transmitters of metabolic signals from the periphery to GnRH neurons (2, 30, 31). Several studies have documented a clear impact of conditions of undernutrition or metabolic stress on *Kiss1* expression in the hypothalamus. Mice subjected to fasting display a significant reduction in hypothalamic *Kiss1* mRNA levels, which precedes the decline in GnRH expression (32). Similarly, chronic subnutrition during puberty has been shown to reduce *Kiss1* mRNA levels in the arcuate nucleus (ARC) in female rats (33). Furthermore, repeated central injections of kisspeptin to female rats with arrested puberty due to chronic subnutrition restored pubertal progression despite the persistent caloric restriction (34). These findings suggest that *Kiss1* neurons may transmit metabolic information provided by insulin levels to GnRH neurons.

Whether *Kiss1* neurons mediate the influence of metabolic factors on the timing of puberty is not clear. Leptin receptors colocalize with *Kiss1* neurons (35), yet we re-

cently showed that leptin's effects on puberty in mice do not require *Kiss1* neurons (36). Using the Cre/loxP system to generate *Kiss1* neuron-specific insulin receptor knockout mice (IR^{ΔKiss}), we have ablated the insulin receptor in *Kiss1* cells to test whether insulin signaling plays a necessary role in the function of *Kiss1* neurons. Lack of insulin signaling in *Kiss1* neurons delayed puberty in both female and male mice in our model but had no effect on adult fertility. Our results show that insulin sensing in *Kiss1* neurons modifies the timing of puberty, thus providing a mechanism that may advance puberty in well-nourished individuals.

Materials and Methods

Animals and genotyping

To generate mice with the IR specifically deleted in *Kiss1* neurons, *Kiss1*-Cre mice (37) were crossed with insulin receptor-floxed mice (10) and bred to homozygosity for the floxed allele only. The IR^{flox/flox} mice were designed with loxP sites flanking exon 4. Excision of exon 4 in the presence of Cre recombinase results in a frameshift mutation and produces a premature stop codon. Littermates lacking Cre expression were used as controls (IR^{flox/flox}). All mice were on a mixed C57BL/6J-129S6/SvEv background. Where specified, the mice also carried the Gt(ROSA)26Sor locus-inserted enhanced green fluorescent protein (EGFP) gene [B6.129-Gt(ROSA)26Sor^{tm2Sho}/J; The Jackson Laboratory, Bar Harbor, Maine], serving as a reporter under the control of Cre recombinase expression. Mice were housed in the University of Toledo College of Medicine animal facility at 22°C to 24°C on a 12-hour light/12-hour dark cycle and were fed standard rodent chow (2016 Teklad Global 16% Protein Rodent Diet, 12% fat by calories; Harlan Laboratories, Indianapolis, Indiana). On postnatal day (PND) 22, mice were weaned if litter size was within 5 to 10 to prevent birth size effects on body weight. At the end of the study, all animals were sacrificed by CO₂ asphyxiation or by cardiac puncture under 2% isoflurane anesthesia to draw blood. All procedures were reviewed and approved by University of Toledo College of Medicine Animal Care and Use Committee. Mice were genotyped as described previously (37, 38). Additional genotyping was performed by Transnetyx, Inc (Cordova, Tennessee) using a real-time PCR-based approach.

Western blotting

Adult mice were sacrificed, and hypothalamus, liver, muscle, visceral adipose tissues, and gonads were harvested. Tissues were snap-frozen in liquid nitrogen and stored at –80°C until homogenized in radioimmunoprecipitation assay lysis buffer (Millipore, Billerica, Massachusetts) supplemented with protease inhibitor and phosphatase inhibitor (Thermo Fisher Scientific, Waltham, Massachusetts). After centrifugation, supernatant protein concentrations were determined by BCA protein assay (Thermo Fisher Scientific). Then 30-μg denatured samples were subjected to SDS-PAGE electrophoresis and Western blotting using IR β subunit (1:1000; Santa Cruz Biotechnology, Inc, Santa Cruz, California). β-Actin (1:1000; Sigma-Aldrich, St Louis, Missouri) or α-tubulin (1:1000; Cell Signaling Technology, Danvers, Massachusetts) was used as a loading control.

Fluorescence-activated cell sorting (FACS)

FACS and RNA extractions were done according to published protocols with minor modifications (37). In brief, 4 female *Kiss1-Cre/EGFP* mice and 4 female *IR^{ΔKiss}* mice (also carrying the EGFP reporter) were sacrificed via cervical dislocation, and intact hypothalami were removed. The hypothalami were placed in cold Hanks' balanced salt solution (without calcium or magnesium; Thermo Fisher Scientific), cut into pieces, and digested by papain (Worthington Biochemical Corporation, Freehold, New Jersey) solution in Hanks' balanced salt solution (1 mg/mL) in a 37°C incubator with 5% CO₂ for 30 minutes with occasional mixing by pipetting. Cells were then centrifuged at 2000g for 5 minutes, and the supernatant was removed. FACS buffer (0.1% bovine serum albumin and 1% EDTA in 1× PBS) was used to stop digestion and resuspend cells. Cells were processed to isolate EGFP-expressing cells via FACS Aria (BD Biosciences, San Jose, California) according to EGFP wavelength. Total RNA was extracted by an Arcturus PicoPure RNA isolation kit (Applied Biosystems, Foster City, California), and RT-PCR was performed for the *IR* cDNA in isolated EGFP-expressing *Kiss1* neurons (Applied Biosystems). *IR* primers were the same as those published previously (32).

Perfusion and immunohistochemistry

Adult male mice and female mice at diestrus at the age of 3 to 6 months were deeply anesthetized by ketamine and xylazine, and then a perfusion needle was inserted into the left ventricle. After brief perfusion with a saline rinse, mice were perfused transcardially with 10% formalin for 10 minutes, and the brain was removed. The brain was postfixed in 10% formalin at 4°C overnight and immersed in 20% sucrose at 4°C for 48 hours. Then 25- μ m sections were cut by a sliding microtome into 5 equal serial sections. Sections were treated with 3% hydrogen peroxide for 30 minutes to quench endogenous peroxidase activity. After rinsing in PBS, sections were blocked for 2 hours in PBS-azide-T (PBS-azide, Triton X-100, and 3% normal donkey serum). Then, samples were incubated for at least 48 hours at 4°C in PBS-azide-T-containing rabbit anti-kisspeptin antibody (1:1000; Millipore), which has been tested for specificity (39). After several washes in PBS, sections were incubated in PBS-T (Triton X-100 and 3% donkey serum) containing biotinylated anti-rabbit IgG (1:1000; Vector Laboratories, Burlingame, California), followed by incubation in ABC reagent (Vector Laboratories) for 60 minutes at room temperature. Sections were washed, and immunoreactivity was visualized by 0.6 mg/mL diaminobenzidine hydrochloride (Sigma-Aldrich) in PBS with hydrogen peroxide. Finally, sections were washed, mounted on slides, dried overnight, dehydrated, cleared, and coverslipped. *Kiss1*-immunoreactive neurons in the AVPV/PeN and ARC were quantified as described previously (39, 40).

Dual-label in situ hybridization/immunofluorescence

Female mice at the age of 4 to 5 months were perfused with diethylpyrocarbonate-treated saline and then formalin ($n = 3$, *Kiss1-Cre/EGFP* and *IR^{ΔKiss}* female mice on diestrus). Dual-label in situ hybridization and immunofluorescence assays were performed as described previously (37, 41). In brief, free-floating hypothalamic sections were treated with 1% sodium borohydride for 15 minutes followed by 0.25% acetic anhydride in 0.1

M triethanolamine (pH 8.0) for 10 minutes. Sections were incubated at 50°C for 12 to 16 hours in hybridization solution (50% formamide; 10 mM Tris-HCl, pH 8.0; 5 mg of tRNA; 10 mM dithiothreitol; 10% dextran sulfate; 0.3 M NaCl; 1 mM EDTA; and 1× Denhardt's solution) containing the previously validated ³³P-labeled *IR* riboprobe diluted to 10⁶ cpm/mL (68). Sections were then washed in 2× sodium citrate/sodium chloride and treated with 0.002% RNase A (Roche Applied Science; Indianapolis, Indiana) for 30 minutes, followed by stringency washes in decreasing concentrations of sodium citrate/sodium chloride. Sections were incubated overnight at room temperature in anti-green fluorescent protein (GFP) (made in chicken, 1:5000; Aves Labs, Tigard, Oregon) primary antibody. On the next day, sections were washed in PBS and then were incubated in Alexa Fluor 488-conjugated goat anti-chicken antibody (1:500) for 2 hours. Sections were mounted onto SuperFrost Plus slides, dehydrated in ethanol, and placed in X-ray film cassettes with BMR-2 film (Kodak, Rochester, New York) for 4 days and then were dipped in NTB-2 photographic emulsion (Kodak), for 4 weeks. Slides were developed with D-19 developer (Kodak), dehydrated in ethanol, cleared in xylenes, and coverslipped with PermaSlip.

Metabolic phenotype assessment

Body weight was measured weekly in a single-occupant cage with ALPHA-dri bedding. Body composition in 4-month-old mice was assessed by nuclear magnetic resonance (minispec mq7.5; Bruker Optics, Billerica, Massachusetts) to determine the percentage of fat mass, as described previously (42). Glucose tolerance tests (GTTs) and insulin tolerance tests (ITTs) were done as described previously (38). In brief, after a 6-hour fast, mice were injected with dextrose (2g/kg ip). Tail blood glucose was measured using a mouse-specific glucometer (AlphaTRAK; Abbott Laboratories, Abbott Park, Illinois) before and 15, 30, 45, 60, 90, and 120 minutes after injection. For ITTs, after a 4-hour fast, mice were injected with recombinant insulin (0.75 U/kg ip). Tail blood glucose was measured again at specified time points. Food intake and indirect calorimetry were measured from female mice at the age of 2 to 3 months in a Calorimetry Module (CLAMS; Columbus Instruments, Columbus, Ohio) as described previously (43).

Puberty and reproductive phenotype assessment

Balanopreputial separation was checked daily from weaning by manually retracting the prepuce with gentle pressure (44). Singly housed female mice were checked daily for vaginal opening after weaning at 3 weeks of age. Vaginal lavages from female mice were collected from the day of vaginal opening for at least 3 weeks. Stages were assessed based on vaginal cytology (45, 46): predominant cornified epithelium indicated the estrous stage, predominant nucleated cells indicated the proestrous stage, and predominant leukocytes indicated the diestrous stage. At the age of 33 days, each male mouse was paired with 1 wild-type female mouse of proven fertility for 4 weeks or until the female mouse was obviously pregnant. Then the paired mice were separated, and the delivery date was recorded. The age of sexual maturation was estimated from the birth of the first litter minus average pregnancy duration for mice (20 days). At 4 to 6 months of age, animals were again paired with wild-type adult breeders to collect additional data on litter size and intervals between litters.

Hormone assays

Submandibular blood was collected at 10:00 to 11:00 AM to detect basal LH and FSH levels using the rat pituitary panel (Millipore) performed by the University of Virginia Center for Research in Reproduction (Charlottesville, Virginia). This time point was chosen to avoid the LH surge in randomly cycling mice. The assay for LH had a detection sensitivity of 3.28 pg/mL. The intra-assay and interassay coefficients of variance (CVs) were 6.9% and 17.2%, respectively. FSH was measured in female mice at diestrus and in male mice. For FSH, the lower limit of detection was 7.62 pg/mL, with intra-assay and interassay CVs of 6.7% and 16.9%. Serum estradiol was measured by ELISA (Calbiotech, Spring Valley, California) with sensitivity of <3 pg/mL and intra-assay and interassay CVs of 3.1% and 9.9%. Serum testosterone was measured by RIA at Oregon Health and Science University Endocrine Technology and Supporting Lab (Beaverton, Oregon) with a sensitivity range of 0.05 to 25 ng/mL and intra-assay and interassay CVs of <10% and <15%. Leptin was measured from random-fed PND 31 mice and adult mice by ELISA (Crystal Chem, Inc, Downers Grove, Illinois) with a sensitivity range of 0.2 to 12.8 ng/mL and intra-assay and interassay CVs of \leq 10%. Serum collected after an overnight fast was used for measurement of insulin (Crystal Chem, Inc) and triglyceride (Pointe Scientific, Canton, Michigan). The insulin ELISA kit had a sensitivity range of 50 to 3200 pg/mL, with both intra-assay and interassay CVs of \leq 10%.

Histology

Ovaries and testes were collected from mice and fixed immediately in 10% formalin overnight. Then tissues were embedded in paraffin and cut into 5- to 8- μ m sections. Sections were stained by hematoxylin and eosin.

Quantitative real-time PCR

Mice were decapitated after isoflurane anesthesia, and brains and other tissues were removed. Total RNA was extracted from dissected tissues by an RNeasy Lipid Tissue Mini Kit (QIAGEN, Valencia, California), and single-strand cDNA was synthesized by a High-Capacity cDNA Reverse Transcription kit (Applied Biosystems) using random hexamers as primers. A 10 μ M cDNA template was used in a 25- μ L system in 96-well plates with SYBR Green qPCR SuperMix/ROX (Smart Bioscience Inc, Maumee, Ohio). Primers for amplification of *Kiss1* mRNA were the same as those in a previous publication (32). Each sample was analyzed in triplicate to measure *Kiss1* expression level. The reactions were run in an ABI PRISM 7000 sequence detection system (PE Applied Biosystems, Foster City, California) and analyzed using the comparative Ct method ($2^{-\Delta\Delta Ct}$) with glyceraldehyde-3-phosphate dehydrogenase as the normalizer.

Ovariectomy (OVX) and acute estradiol benzoate (EB) treatment

Female mice, 2 to 4 months of age, were anesthetized by ketamine and xylazine (9:00 AM–12:00 PM), and blood samples were collected submandibularly immediately before OVX. Seven to 14 days later, blood samples were collected again at the same time of day. Mice were then subcutaneously injected with 10 μ g/mouse EB (Sigma-Aldrich) in sesame oil, and 2 hours after injection, blood samples were obtained for measurement of LH.

Data analysis and production of digital images

Brain sections were visualized with a Zeiss Axioskop2 microscope. Photomicrographs were produced by capturing images with a Zeiss Axiocam HRc digital camera and AxioVision software. Only the sharpness, contrast, and brightness were adjusted. Quantification of dual-labeled neurons and percentage of colocalization were determined in the AVPV and in 2 rostro-caudal levels of the ARC. Cells were counted in one side of a determined level of each nucleus. We considered cells dual-labeled if the density of silver grains (^{33}P -labeled riboprobe) overlying a green fluorescent cytoplasm was at least 3 times that observed in the background. For background determination, we used the density of silver grains overlying the superior cerebellar peduncle, where no cell bodies were detected.

Statistical analysis

Data are presented as means \pm SEM. Two-tailed unpaired *t* testing was used as the main statistical method. The Mann-Whitney *U* test was used if the data did not assume a normal distribution. One-way ANOVA was performed to compare the 3 groups, followed by the Bonferroni multiple comparison test. For body weight, GTTs, and ITTs, repeated-measures ANOVA was used to compare changes over time between 2 genotypes. A value of *P* < .05 was considered to be significant.

Results

To generate mice with the IR specifically deleted in *Kiss1* neurons, we crossed IR^{flox/flox} mice (47) with *Kiss1*-Cre mice (37) carrying the Cre recombinase gene driven by the *Kiss1* promoter. To verify that the IR gene was excised in *Kiss1* neurons, PCR was performed on DNA from different tissues. As expected, a 500-bp band indicating gene deletion was produced from the hypothalamus and other tissues expressing *Kiss1*, including cerebrum, ovary, testis, liver, and pancreas (Figure 1A) (37, 48). However, *Kiss1* expression levels in liver and pancreas were low by real-time PCR (Figure 1B). IR protein levels were similar between wild-type and targeted-knockout liver, muscle, visceral adipose tissue, testis, and ovary (Figure 1C). Consistent with restriction of IR inactivation to a defined subpopulation of hypothalamic neurons, Western blot analysis revealed no alteration of IR expression in hypothalamus (data not shown) (49). Thus, insulin sensing appears to be intact in most cells in the ovary and other tissues.

Kisspeptin neurons express insulin receptors

To examine expression of IRs specifically in *Kiss1* neurons, these neurons were isolated by FACS sorting from EGFP reporter mice. RT-PCR of *Kiss1*-EGFP neurons showed an IR band in wild-type but not in IR ^{Δ Kiss} mice, indicating that IRs are present in *Kiss1* neurons and are deleted successfully in IR ^{Δ Kiss} mice (Figure 1D). Further-

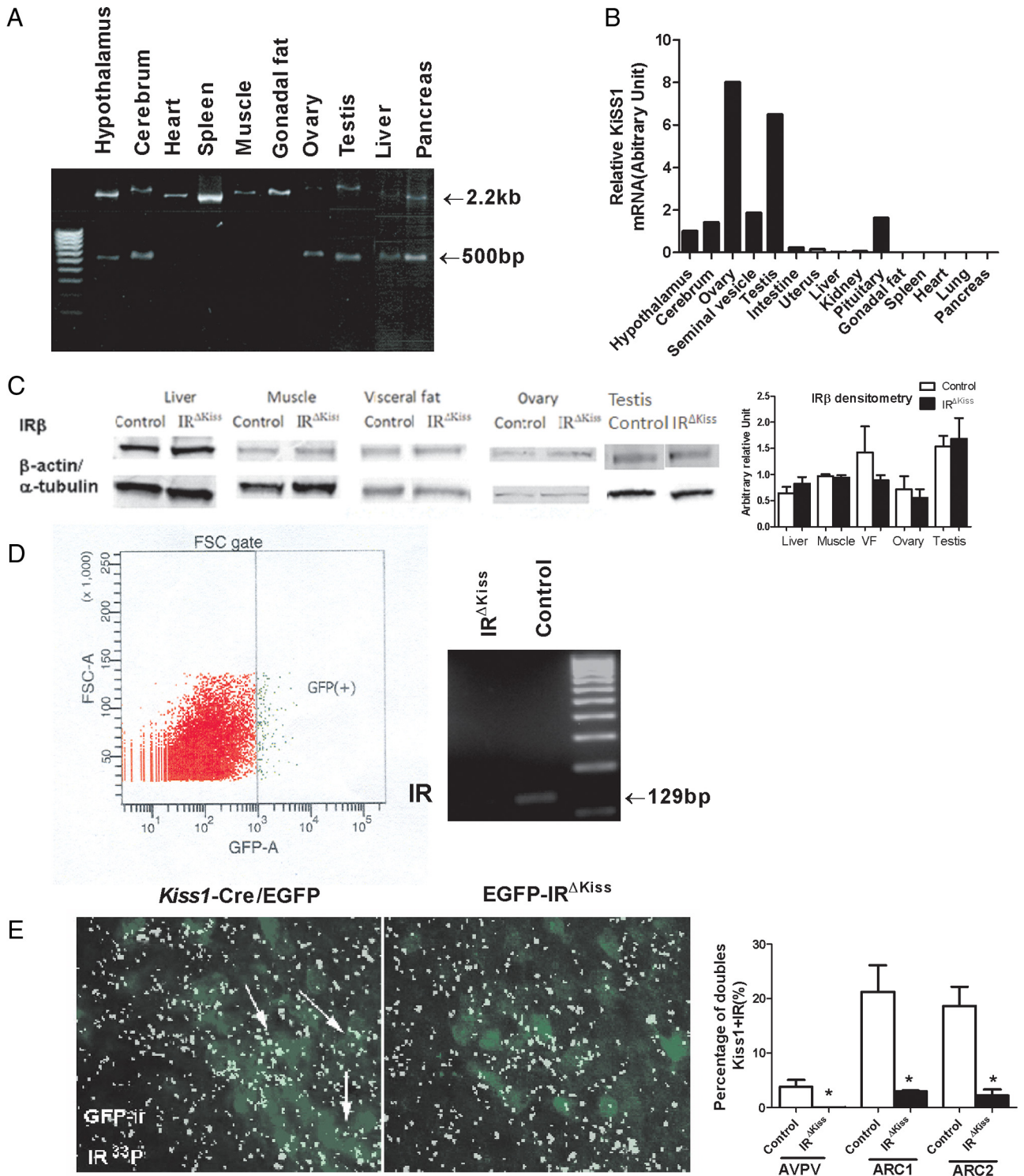


Figure 1. Generation of IR^{ΔKiss} mice. A, PCR of DNA from different tissues. The excised IR gene appears as a 500-bp band and the unexcised IR gene sequence as a 2.2-kb band. B, *Kiss1* expression in different tissues in a wild-type female by real-time PCR. C, IRβ expression in different tissues and densitometry (n = 3-5 in each group). D, FACS and RT-PCR of IRs from GFP-positive cells isolated from 4 control female reporter mice (no IR^{fllox/fllox}) and 4 female reporter IR^{ΔKiss} mice. E, Colocalization of *Kiss1* neuron and IRs and quantification of double staining percentages from female control and IR^{ΔKiss} mice in the AVPV and ARC (n = 3). *P < .05.

more, dual-label in situ hybridization/immunofluorescence showed that approximately 22% *Kiss1* neurons in the ARC were colocalized with IRs in wild-type mice, whereas the percentage was sharply reduced to about 2%

in knockout mice (Figure 1E). Interestingly, in the AVPV, only 3% to 5% *Kiss1* colocalized with IRs in wild-type mice. No colocalization was found in the AVPV of IR^{ΔKiss} mice (Figure 1E).

IR^{ΔKiss} mice have a normal metabolic phenotype

Because of the potential interaction between *Kiss1* neurons and metabolic circuits in the hypothalamus, we examined the metabolic phenotype of IR^{ΔKiss} mice. The body weights of both female and male mice showed no significant difference between control and knockout mice (Figure 2, A and B); 48-hour food intake was comparable between the 2 groups in 2- to 3-month-old females (Figure 2C). Fat mass, lean mass, and fat percentage were comparable in both females and males (Figure 2, D and E). Serum insulin was not statistically different between control and IR^{ΔKiss} mice of both sexes (Figure 2, F and G), suggesting that β -cell insulin secretion is normal in these mice. Furthermore, glucose tolerance was normal in both sexes of IR^{ΔKiss} mice (Figure 2, H and I). No significant differences were seen in visceral fat weight, serum triglyceride levels, or leptin levels at PND 31 and adulthood.

Moreover, energy expenditure, oxygen consumption, and insulin tolerance did not differ between control and IR^{ΔKiss} adult mice (data not shown).

Female IR^{ΔKiss} mice experience delayed puberty with normal fertility

To assess the progression of puberty in female mice, we measured vaginal opening and timing of the first entrance into estrus. In female mice, vaginal opening indicates the activation of the hypothalamic-pituitary-gonadal (HPG) axis at puberty (50). Female IR^{ΔKiss} mice experienced vaginal opening approximately 3 days later than control mice (PND 31.4 \pm 0.5 vs PND 34.0 \pm 0.9) (Figure 3A). The day of first estrus implies the establishment of the hormonal cyclicity necessary for female reproduction (50). The age of first estrus was also significantly postponed in IR^{ΔKiss} mice (PND 39.6 \pm 1.2 vs PND 44.1 \pm 1.6, Figure 3B). LH

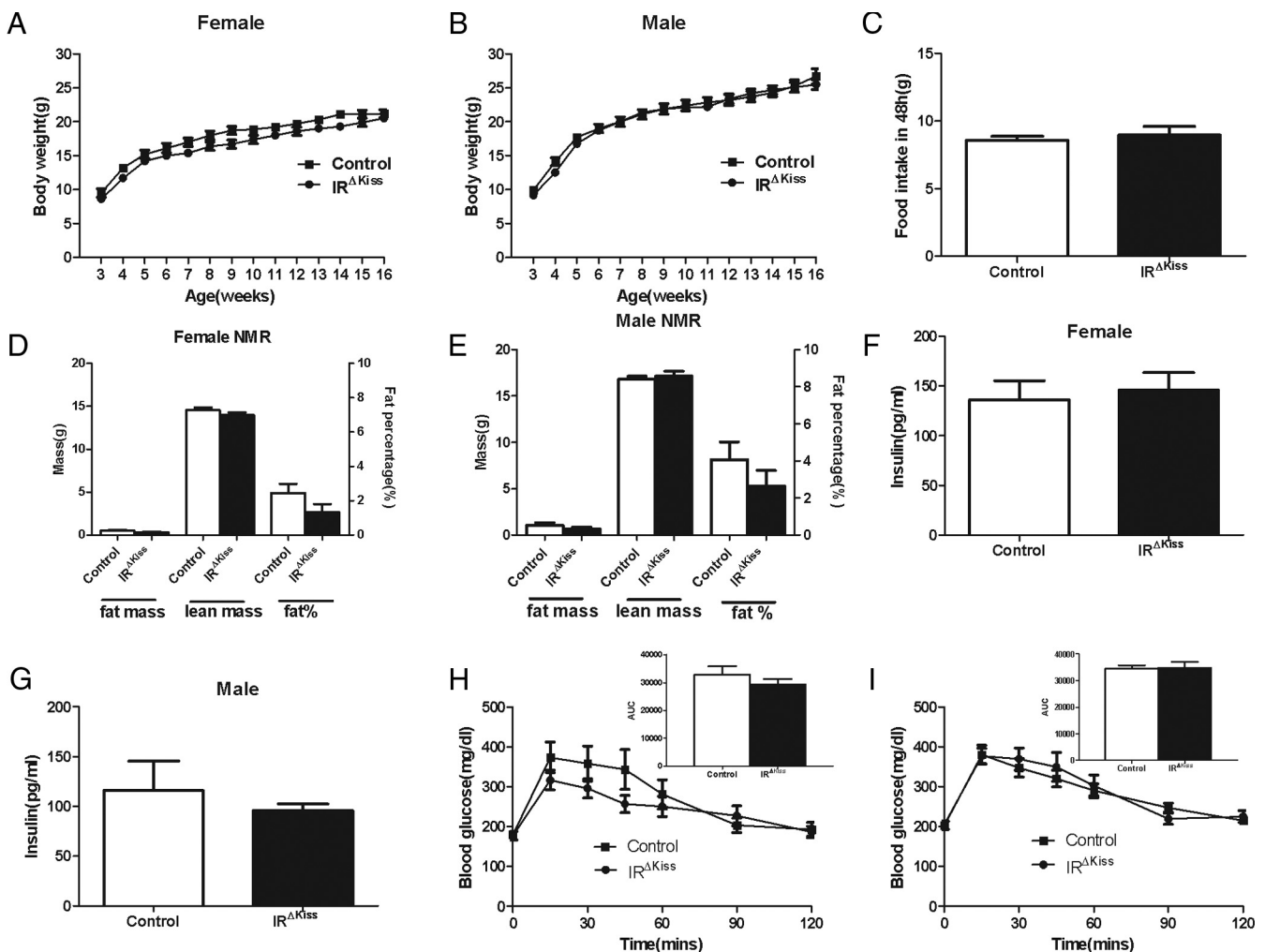


Figure 2. Normal metabolic phenotype in adult IR^{ΔKiss} mice. A, Weekly body weight of female mice (n = 13 each group). B, Weekly body weight of male mice (n = 16 each group). C, 48-hour food intake measured by calorimetric cages. D, Female body composition at the age of 4 months in control (n = 16) and IR^{ΔKiss} (n = 14) mice. E, Male body composition at the age of 4 months in control (n = 10) and IR^{ΔKiss} (n = 8) mice. F, Female serum insulin at the age of 4 to 6 months in control (n = 9) and IR^{ΔKiss} (n = 10) mice. G, Male serum insulin at the age of 4 to 6 months in control (n = 11) and IR^{ΔKiss} (n = 10) mice. H, GTT and area under the curve (AUC) (inset) in 2- to 3-month old female control (n = 9) and IR^{ΔKiss} (n = 10) mice. I, GTT and AUC (inset) in 2- to 3-month old male control (n = 18) and IR^{ΔKiss} (n = 13) mice. NMR, nuclear magnetic resonance.

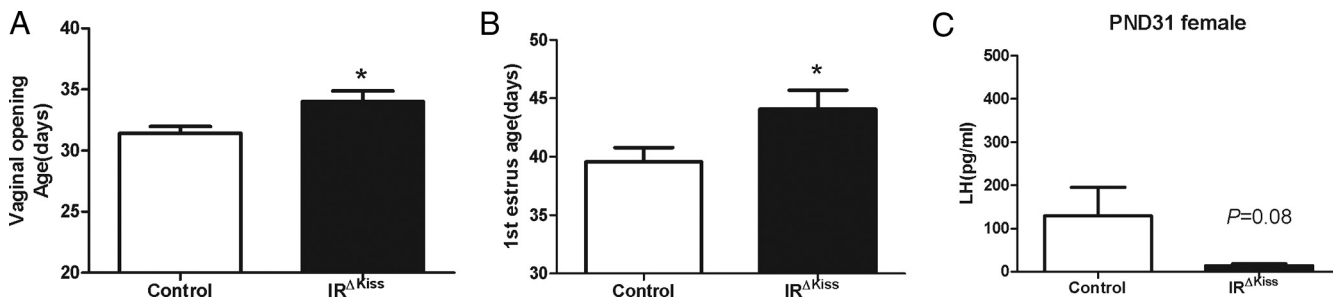


Figure 3. Delayed puberty in female $IR^{\Delta KISS}$ mice. A, Vaginal opening was evaluated in control (n = 12) and $IR^{\Delta KISS}$ (n = 10) mice. B, First estrus was evaluated in control (n = 9) and $IR^{\Delta KISS}$ (n = 10) mice. C, LH on PND 31 in control (n = 11) and $IR^{\Delta KISS}$ (n = 10) mice. * $P < .05$.

levels in $IR^{\Delta KISS}$ mice trended lower than those in controls on PND 31 (Figure 3C), whereas estradiol was comparable between the 2 groups on PND 31 (control, 5.2 ± 0.6 pg/mL, n = 10 vs $IR^{\Delta KISS}$, 5.2 ± 0.6 pg/mL, n = 11). However, LH, FSH, and estradiol were comparable between the 2 groups in adulthood (Figure 4, A–C). Female knockout mice also had normal estrous cyclicity, characterized by normal estrous length and staging (Figure 4D). In addition, adult female $IR^{\Delta KISS}$ mice had similar ovary and uterus weights (data not shown). Ovarian morphology showed follicles at all stages of maturation and comparable numbers of corpora lutea between control and knockout mice (Figure 4E). At 4 to 6 months of age, mice were paired with established wild-type male breeders. Both the latency to birth and litter size were comparable between the 2 groups (Figure 4F).

Male $IR^{\Delta KISS}$ have delayed puberty with normal fertility

Testis mass in $IR^{\Delta KISS}$ mice was lower than that of controls, indicating a delay of gonadal development (Figure 5A). Balanopreputal separation is an indicator of activa-

tion of the reproductive axis in males (44). However, this measure showed no difference between the 2 groups (Figure 5B), nor did testosterone levels differ on PND 25 (control, 0.6 ± 0.1 ng/mL, n = 10 vs $IR^{\Delta KISS}$, 0.6 ± 0.1 ng/mL, n = 7) or PND 31 (control, 1.1 ± 0.3 ng/mL, n = 10 vs $IR^{\Delta KISS}$, 1.6 ± 0.5 ng/mL, n = 8). Nevertheless, LH levels in $IR^{\Delta KISS}$ mice were lower than those of controls on PND 31 (Figure 5C). Finally, the age of sexual maturation, as measured by the age at which each male mouse was able to impregnate a female mouse of known fertility, was significantly delayed compared with that of controls (43.7 ± 2.2 vs 49.4 ± 1.1 days) (Figure 5D).

In adults, LH, FSH, and testosterone were not statistically different between the 2 groups (Figure 6, A–C). Furthermore, the testis weight was normal in adult $IR^{\Delta KISS}$ mice (data not shown). Testis histology showed all stages of spermatogenesis in seminiferous tubules and normal interstitial Leydig cells in $IR^{\Delta KISS}$ mice (Figure 6D). Fertility at 4 to 6 months of age, characterized by litter size and days required to impregnate a female, was not different between control and $IR^{\Delta KISS}$ male mice (Figure 6E).

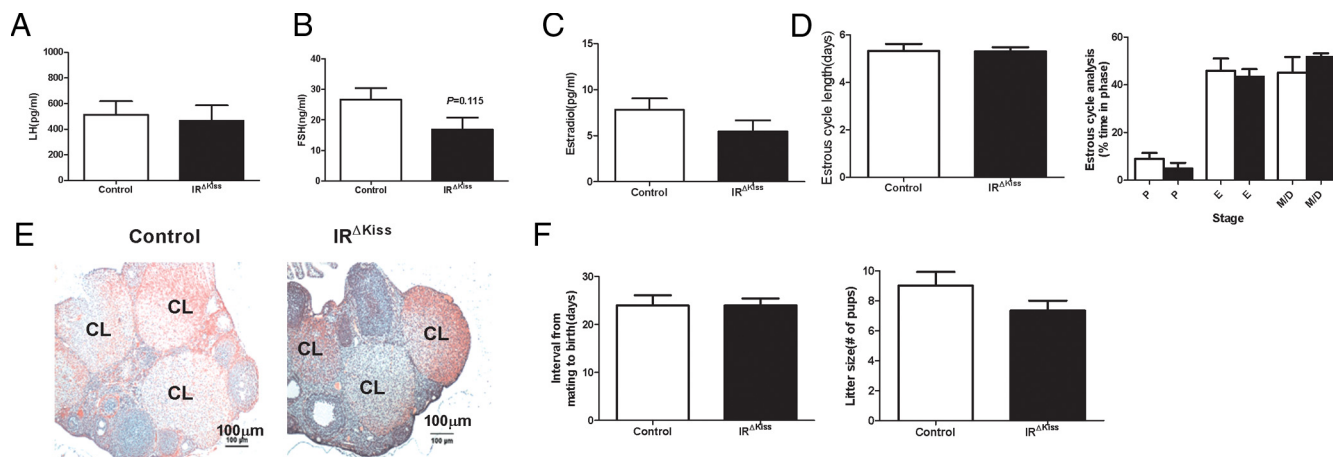


Figure 4. Normal female reproduction in adult $IR^{\Delta KISS}$ mice. A, Basal LH levels in adult female control (n = 16) and $IR^{\Delta KISS}$ (n = 18) mice. B, Basal FSH levels in adult female control (n = 5) and $IR^{\Delta KISS}$ (n = 4) mice. C, Estradiol in adult female control (n = 9) and $IR^{\Delta KISS}$ (n = 10) mice. D, Estrous cycle length (control, n = 9; $IR^{\Delta KISS}$, n = 13) and estrous cycle analysis (control, n = 5; $IR^{\Delta KISS}$, n = 7) in 7- to 10-week-old females. E, Representative light photomicrographs of adult ovaries in control and $IR^{\Delta KISS}$ mice (n = 4). CL, corpora lutea. Scale bar corresponds to 100 μ m. F, Fertility data from 4- to 6-month-old females paired with established male breeders. The interval from mating to birth of a litter and litter size were compared between control (n = 8) and $IR^{\Delta KISS}$ (n = 12) mice.

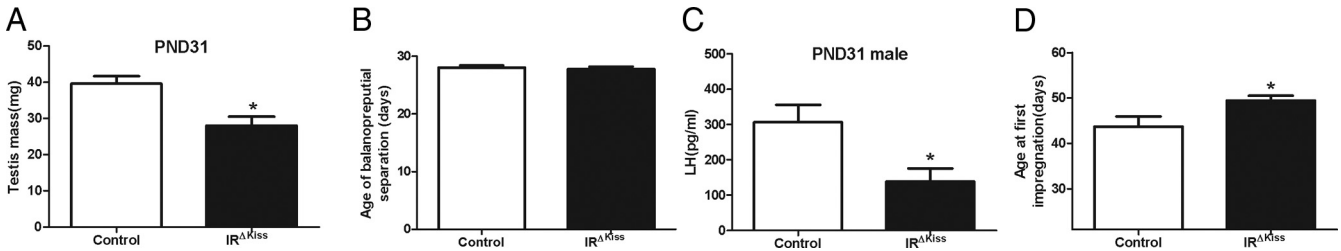


Figure 5. Delayed male puberty in $IR^{\Delta Kiss}$ mice. A, Testis mass (control, $n = 5$; $IR^{\Delta Kiss}$, $n = 4$). B, Normal balanopreputial separation age (control, $n = 12$; $IR^{\Delta Kiss}$, $n = 10$). C, LH on PND 31 in control ($n = 6$) and $IR^{\Delta Kiss}$ ($n = 5$) mice. D, Estimated age of first impregnation calculated by subtraction of 20 days from the time required for delivery of a litter (control, $n = 8$; $IR^{\Delta Kiss}$, $n = 10$). * $P < .05$.

***Kiss1* expression during puberty**

We counted the *Kiss1* neuron numbers in the AVPV/PeN and measured the *Kiss1* immunoreactive areas in the ARC from PND 31 mice (Figure 7, A–D). In PND 31 females, *Kiss1* neuron numbers in the AVPV/PeN in $IR^{\Delta Kiss}$ mice were fewer than those in the wild-type mice, whereas the numbers in the ARC *Kiss1* neuron immunoreactive area were similar between the 2 groups (Figure 7C). In PND 31 males, *Kiss1* neuron numbers in the AVPV/PeN did not differ, and the *Kiss1* immunoreactive area was similar in the ARC between the 2 groups (Figure 7D). In adults, normal patterns of kisspeptin staining were seen in both AVPV/PeN and ARC (Figure 7, E–H).

$IR^{\Delta Kiss}$ mice have a normal response to estrogen feedback

The secretion of GnRH in adulthood is regulated by feedback of gonadal sex steroids, and hypothalamic *Kiss1* neurons may play a role in transmitting steroid feedback signals to the reproductive axis (51). In addition, insulin and estrogens can activate shared intracellular signaling

pathways (52). We therefore investigated the possibility that insulin action in *Kiss1* neurons participates in the negative feedback that estrogens exert on GnRH neurons. Mice were ovariectomized and then treated with EB. LH was significantly increased after OVX and suppressed by administration of EB similarly in both $IR^{\Delta Kiss}$ mice and control animals. Contrary to the above hypothesis, the baseline, OVX, and OVX plus EB animals did not differ between the 2 groups (Figure 8).

Discussion

Hyperinsulinemia is widely believed to advance pubertal maturation (53). Insulin increases in children around the time of adrenarche, in association with increasing adiposity, circulating IGF-1, and insulin resistance in peripheral tissues (54). Indeed, reduction of insulin levels by metformin administration in girls with precocious pubarche resulted in a delay in the clinical onset of puberty (55). Likewise, metformin blocked the ability of a high-fat diet

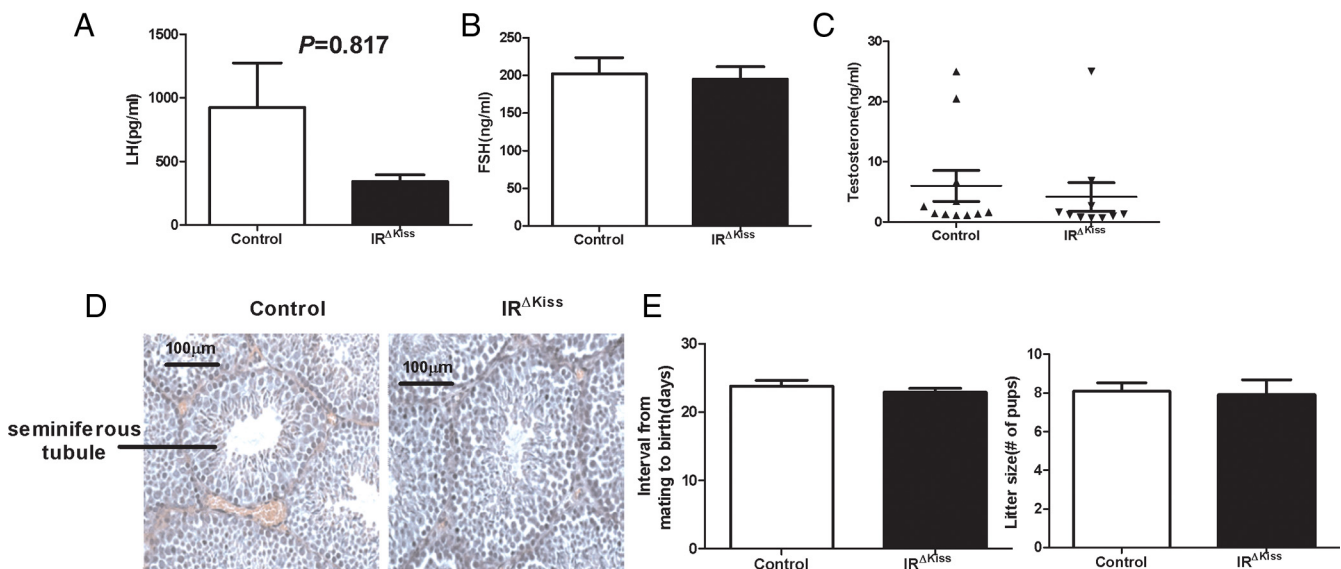


Figure 6. Normal male reproduction in adult $IR^{\Delta Kiss}$ mice. A, LH in adult male control and $IR^{\Delta Kiss}$ mice ($n = 9$). B, FSH in adult male control ($n = 10$) and $IR^{\Delta Kiss}$ ($n = 9$) mice. C, Testosterone in adult male control ($n = 11$) and $IR^{\Delta Kiss}$ ($n = 10$) mice. D, Representative sections of adult testis in control and $IR^{\Delta Kiss}$ mice ($n = 4$). Scale bar corresponds to 100 μm . E, Fertility data from 4- to 6-month-old males paired with established female breeders. Interval from mating to birth of a litter and litter size were compared between control and $IR^{\Delta Kiss}$ mice ($n = 11$).

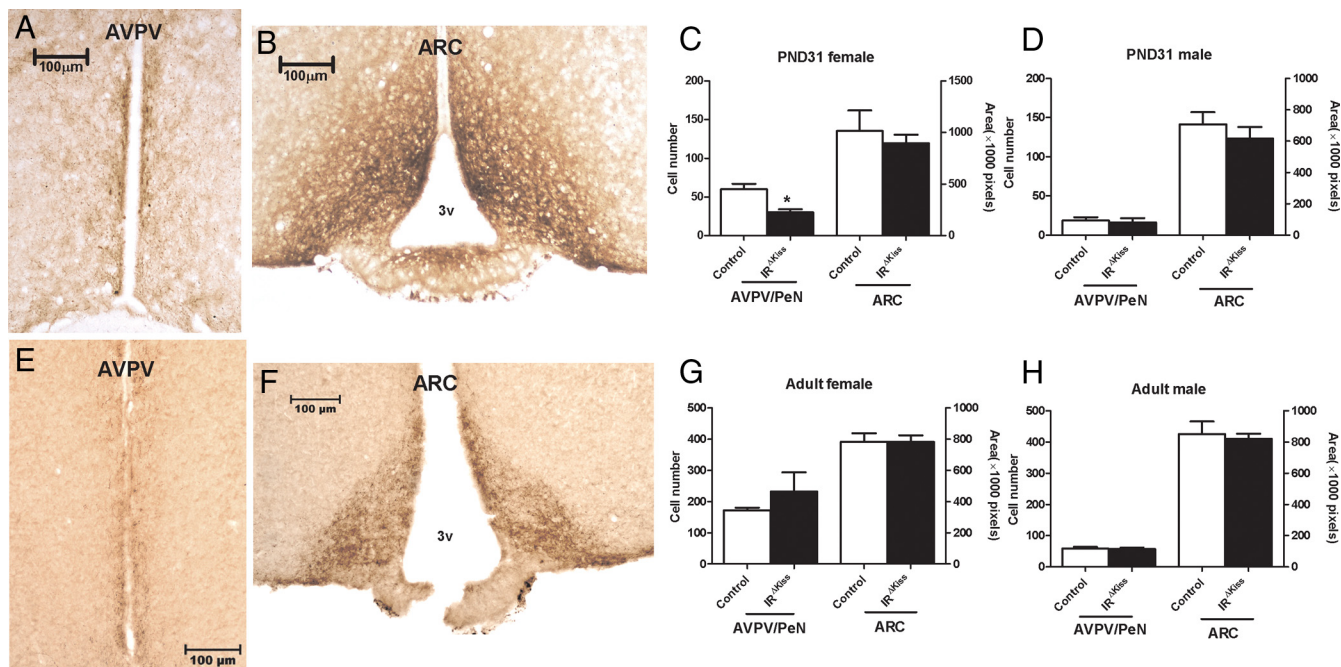


Figure 7. Reduced *Kiss1* cell number in the AVPV/PeN in juvenile $IR^{\Delta Kiss}$ female mice. A, and B, Representative micrograph showing *Kiss1* immunostaining in the AVPV and ARC in a female $IR^{\Delta Kiss}$ mouse on PND 31. C, Quantification of *Kiss1* cell numbers in the AVPV/PeN and *Kiss1* immunoreactive area in the ARC in PND 31 females (control, n = 3; $IR^{\Delta Kiss}$, n = 5). D, Quantification of *Kiss1* cell numbers in the AVPV/PeN and *Kiss1* immunoreactive area in the ARC in PND 31 males (control, n = 4; $IR^{\Delta Kiss}$, n = 3). E and F, Representative immunostaining micrograph for kisspeptin in the AVPV and ARC in an adult female $IR^{\Delta Kiss}$ mouse. G, Quantification of *Kiss1* cell numbers in the AVPV/PeN and *Kiss1* immunoreactive area in the ARC in adult females (n = 3). H, Quantification of *Kiss1* cell numbers in the AVPV/PeN and *Kiss1* immunoreactive area in the ARC in adult males (n = 3). * $P < .05$.

to advance puberty in mice (56). These effects may result in part from insulin inducing increased GnRH production. Increasing circulating insulin levels in adult male mice with hyperinsulinemic clamp studies induces a significant rise in LH secretion (8). In women, hyperinsulinemic clamping likewise resulted in significant increases in the frequency of LH pulsatility (57), although this effect was not found in men (58). Furthermore, mice that lack insulin signaling in the brain (NIRKO mice) have low LH levels that increase in response to GnRH, suggesting dysfunction

at the hypothalamic level (10). Male pubertal timing has not been reported in these mice, but NIRKO females exhibit a delay in vaginal opening of 3 to 4 days compared with their littermates (11).

In this study, we have further defined the role of the insulin in the central control of reproduction, demonstrating that insulin signaling in *Kiss1* neurons is crucial for the normal timing of pubertal onset. The delayed pubertal onset was due to hypothalamic-pituitary dysfunction, because female $IR^{\Delta Kiss}$ mice had lower gonadotropin levels than control mice during the pubertal transition. Thus, elimination of insulin signaling by kisspeptin neurons completely recapitulated the effect of neuronal insulin deletion on puberty in female mice. For male mice, measures of maturation of the external genitalia were mixed. However, a functional test of when $IR^{\Delta Kiss}$ mice are able to impregnate a female showed a clear delay. $IR^{\Delta Kiss}$ mice eventually experienced pubertal onset, suggesting that insulin pathway activation in *Kiss1* neurons is ultimately not required for GnRH activation. Clearly, GnRH activation at puberty is dependent on a spectrum of converging genetic, developmental, and environmental signals. Such signals appear to overcome loss of IR activation to eventually induce GnRH pulse generator activity. Likewise, the normal reproductive parameters in adult $IR^{\Delta Kiss}$ mice suggest that other neuronal groups may mediate insulin’s actions

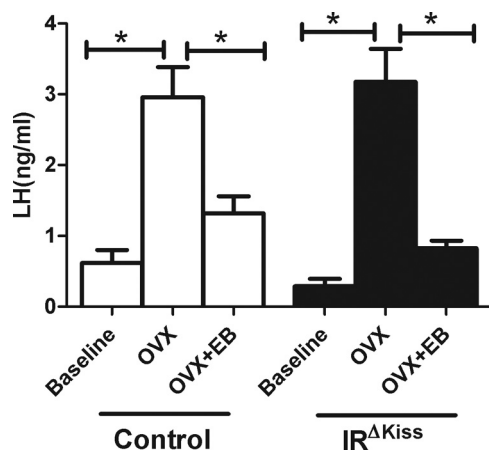


Figure 8. Normal response to estrogen feedback in $IR^{\Delta Kiss}$ mice. Serum LH from intact, OVX, and OVX/EB-injected (2 hours) females in the morning (control, n = 9; $IR^{\Delta Kiss}$, n = 10). * $P < .05$.

on fertility in mature mice. Alternatively, the infertility of adult NIRKO mice may be due to their metabolic derangements, including insulin and leptin resistance and hypertriglyceridemia, rather than the loss of IRs in neurons.

Insulin signaling in the central nervous system has been shown to play an important role in regulation of metabolism and energy balance (10). NIRKO mice show increased food intake and diet-sensitive obesity with increases in body fat, hyperleptinemia, elevated plasma insulin levels, and hypertriglyceridemia. In addition, some evidence suggests that *Kiss1* neurons can interact with the hypothalamic circuitry controlling energy homeostasis (59, 60). In the current study, no abnormality was seen in body weight, visceral fat weight, and serum insulin levels in mice lacking insulin receptors in *Kiss1* neurons. Other metabolic parameters, such as food intake, serum triglyceride, serum leptin, glucose tolerance, and insulin tolerance, were also normal in IR^{ΔKiss} mice. These findings suggest that insulin's role in the brain regulating energy disposal and fuel metabolism is not dependent on *Kiss1* neurons. Although we found no evidence of decreased insulin receptor expression in peripheral tissues, we did not analyze subpopulations of *Kiss1*-expressing peripheral cells (48). Nevertheless, our findings also suggest that insulin signaling in these cells is not required for normal glucose homeostasis. These findings are in accord with previous studies in *Kiss1* knockout mice, in which no abnormal metabolic phenotype was detected (61).

Estrogens act on *Kiss1* neurons to assist in the temporal coordination of juvenile GnRH restraint and subsequent pubertal activation (62), although significant species differences exist in the kisspeptin system (61). In rodents, *Kiss1* neurons are direct targets for the action of sex steroids (62), and the expression of *Kiss1* in the brain is strongly regulated by steroids (63). Regulation of *Kiss1* neurons by an estrogen response element-independent nonclassic estrogen receptor pathway was found in the ARC of mice (64). Intriguingly, both insulin signaling and the nonclassic estrogen receptor pathway are coupled to phosphatidylinositol 3-kinase intracellular signaling in the hypothalamus (52, 65). We therefore considered the possibility that insulin signaling in *Kiss1* neurons can also influence sex steroids signaling in *Kiss1* neurons and in such a way to modify the sex steroid feedback in *Kiss1* neurons. To identify whether insulin's action in *Kiss1* neurons plays a role in estrogen negative feedback, we ovariectomized adult female mice and treated them with EB. Because EB fully suppressed LH production, it appears that insulin sensing by *Kiss1* neurons does not affect the negative feedback of estrogen on these neurons and the HPG axis.

Substantial amounts of evidence support a role for kisspeptin neurons as gatekeepers of puberty (66), but some unanswered questions remain. Although ablation of *Kiss1*

neurons during the late infantile period disrupts the onset of puberty, congenital ablation of 97% of *Kiss1* neurons does not prevent pubertal maturation (67). It therefore appears that a significant amount of developmental compensation is possible, allowing a small number of *Kiss1* neurons or other neuronal circuits to drive pubertal maturation. Given the congenital nature of the targeted ablation we have described here, our results may underestimate the importance of insulin signaling in *Kiss1* neurons in the juvenile or adult animal if a similar process of compensation occurred in our mice. Nevertheless, it should be noted that the overall number of *Kiss1* neurons in adult IR^{ΔKiss} mice was not altered. Another question that remains unanswered is the role of ARC vs AVPV *Kiss1* neurons in the control of puberty. Given that we found most insulin receptors in the *Kiss1* population in the ARC, our results support a role for this population in the modulation of pubertal timing.

In sum, insulin signaling in *Kiss1* neurons is necessary for well-timed activation of the HPG axis during puberty. In contrast, insulin signaling in *Kiss1* cells is unnecessary for normal adult reproductive or metabolic functions. This mechanism may play a role in promoting pubertal development in the presence of abundant energy stores and retarding puberty when the nutritional environment is unfavorable.

Acknowledgments

We thank Dr. Raymond Bourey, Dr. Nikolai Modyanov, Laura Nedorezov, Dr. Sara DiVall, and Lance Stechschulte for their technical assistance with these studies. We also thank the University of Virginia Center for Research in Reproduction Ligand Assay and Analysis Core, supported by Eunice Kennedy Shriver National Institute of Child Health and Human Development/National Institutes of Health (SCCPIR) Grant U54-HD28934.

Address all correspondence and requests for reprints to: Jennifer W. Hill, PhD, Department of Physiology and Pharmacology, University of Toledo College of Medicine, 3000 Transverse Drive, MS 1008, Toledo, Ohio 43614. E-mail: JenniferW.Hill@utoledo.edu.

This work was supported by National Institutes of Health Grants R00HD056491 and R21HD071529 and by a deArce-Koch Fund award (to J.W.H.).

Disclosure Summary: The authors have nothing to disclose.

References

1. Sisk CL, Foster DL. The neural basis of puberty and adolescence. *Nat Neurosci*. 2004;7:1040–1047.
2. Fernandez-Fernandez R, Martini AC, Navarro VM, et al. Novel

- signals for the integration of energy balance and reproduction. *Mol Cell Endocrinol.* 2006;255:127–132.
3. Klentrou P, Plyley M. Onset of puberty, menstrual frequency, and body fat in elite rhythmic gymnasts compared with normal controls. *Br J Sports Med.* 2003;37:490–494.
 4. Bronson FH, Heideman PD. Short-term hormonal responses to food intake in peripubertal female rats. *Am J Physiol.* 1990;259:R25–R31.
 5. Nathan BM, Palmert MR. Regulation and disorders of pubertal timing. *Endocrinol Metab Clin North Am.* 2005;34:617–641, ix.
 6. Woods SC, Lotter EC, McKay LD, Porte D Jr. Chronic intracerebroventricular infusion of insulin reduces food intake and body weight of baboons. *Nature.* 1979;282:503–505.
 7. Schwartz MW, Figlewicz DP, Baskin DG, Woods SC, Porte D Jr. Insulin in the brain: a hormonal regulator of energy balance. *Endocr Rev.* 1992;13:387–414.
 8. Burcelin R, Thorens B, Glauser M, Gaillard RC, Pralong FP. Gonadotropin-releasing hormone secretion from hypothalamic neurons: stimulation by insulin and potentiation by leptin. *Endocrinology.* 2003;144:4484–4491.
 9. Salvi R, Castillo E, Voirol MJ, et al. Gonadotropin-releasing hormone-expressing neurons immortalized conditionally are activated by insulin: implication of the mitogen-activated protein kinase pathway. *Endocrinology.* 2006;147:816–826.
 10. Brüning JC, Gautam D, Burks DJ, et al. Role of brain insulin receptor in control of body weight and reproduction. *Science.* 2000;289:2122–2125.
 11. Gautam DC. 2002 *Analysis of Insulin Receptor Function in the Central Nervous System by Conditional Inactivation of Its Gene in Mice* [PhD thesis]. Cologne, Germany: University of Cologne. <http://d-nb.info/96492353X/34>.
 12. Kovacs P, Morales JC, Karkanias GB. Central insulin administration maintains reproductive behavior in diabetic female rats. *Neuroendocrinology.* 2003;78:90–95.
 13. Steger RW, Kienast SG, Pillai S, Rabe M. Effects of streptozotocin-induced diabetes on neuroendocrine responses to ovariectomy and estrogen replacement in female rats. *Neuroendocrinology.* 1993;57:525–531.
 14. Steger RW, Kienast SG. Effect of continuous versus delayed insulin replacement on sex behavior and neuroendocrine function in diabetic male rats. *Diabetes.* 1990;39:942–948.
 15. Griffin ML, South SA, Yankov VI, Booth RA Jr, Asplin CM, Veldhuis JD, Evans WS. Insulin-dependent diabetes mellitus and menstrual dysfunction. *Ann Med.* 1994;26:331–340.
 16. Elamin A, Hussein O, Tuveno T. Growth, puberty, and final height in children with type 1 diabetes. *J Diabetes Complications.* 2006;20:252–256.
 17. Kim HH, DiVall SA, Deneau RM, Wolfe A. Insulin regulation of GnRH gene expression through MAP kinase signaling pathways. *Mol Cell Endocrinol.* 2005;242:42–49.
 18. DiVall SA, Radovick S, Wolfe A. Egr-1 binds the GnRH promoter to mediate the increase in gene expression by insulin. *Mol Cell Endocrinol.* 2007;270:64–72.
 19. Divall SA, Williams TR, Carver SE, et al. Divergent roles of growth factors in the GnRH regulation of puberty in mice. *J Clin Invest.* 2010;120:2900–2909.
 20. Navarro VM, Castellano JM, Fernandez-Fernandez R, et al. Developmental and hormonally regulated messenger ribonucleic acid expression of KiSS-1 and its putative receptor, GPR54, in rat hypothalamus and potent luteinizing hormone-releasing activity of KiSS-1 peptide. *Endocrinology.* 2004;145:4565–4574.
 21. Shahab M, Mastronardi C, Seminara SB, Crowley WF, Ojeda SR, Plant TM. Increased hypothalamic GPR54 signaling: a potential mechanism for initiation of puberty in primates. *Proc Natl Acad Sci USA.* 2005;102:2129–2134.
 22. Clarkson J, Herbison AE. Postnatal development of kisspeptin neurons in mouse hypothalamus; sexual dimorphism and projections to gonadotropin-releasing hormone neurons. *Endocrinology.* 2006;147:5817–5825.
 23. d'Anglemont de Tassigny X, Fagg LA, Dixon JP, Day K, Leitch HG, Hendrick AG, Zahn D, Franceschini I, Caraty A, Carlton MB, Aparicio SA, Colledge WH. Hypogonadotropic hypogonadism in mice lacking a functional Kiss1 gene. *Proc Natl Acad Sci USA.* 2007;104:10714–10719.
 24. Lapatto R, Pallais JC, Zhang D, et al. Kiss1^{-/-} mice exhibit more variable hypogonadism than Gpr54^{-/-} mice. *Endocrinology.* 2007;148:4927–4936.
 25. de Roux N, Genin E, Carel JC, Matsuda F, Chaussain JL, Milgrom E. Hypogonadotropic hypogonadism due to loss of function of the KiSS1-derived peptide receptor GPR54. *Proc Natl Acad Sci USA.* 2003;100:10972–10976.
 26. Seminara SB, Messager S, Chatzidaki EE, et al. The GPR54 gene as a regulator of puberty. *N Engl J Med.* 2003;349:1614–1627.
 27. Topaloglu AK, Tello JA, Kotan LD, et al. Inactivating KiSS1 mutation and hypogonadotropic hypogonadism. *N Engl J Med.* 2012;366:629–635.
 28. Pineda R, Garcia-Galiano D, Roseweir A, et al. Critical roles of kisspeptins in female puberty and preovulatory gonadotropin surges as revealed by a novel antagonist. *Endocrinology.* 2010;151:722–730.
 29. Navarro VM, Fernandez-Fernandez R, Castellano JM, et al. Advanced vaginal opening and precocious activation of the reproductive axis by KiSS-1 peptide, the endogenous ligand of GPR54. *J Physiol.* 2004;561:379–386.
 30. Dungan HM, Clifton DK, Steiner RA. Minireview: kisspeptin neurons as central processors in the regulation of gonadotropin-releasing hormone secretion. *Endocrinology.* 2006;147:1154–1158.
 31. Forbes S, Li XF, Kinsey-Jones J, O'Byrne K. Effects of ghrelin on Kisspeptin mRNA expression in the hypothalamic medial preoptic area and pulsatile luteinizing hormone secretion in the female rat. *Neurosci Lett.* 2009;460:143–147.
 32. Luque RM, Kineman RD, Tena-Sempere M. Regulation of hypothalamic expression of KiSS-1 and GPR54 genes by metabolic factors: analyses using mouse models and a cell line. *Endocrinology.* 2007;148:4601–4611.
 33. Roa J, Garcia-Galiano D, Varela L, et al. The mammalian target of rapamycin as novel central regulator of puberty onset via modulation of hypothalamic Kiss1 system. *Endocrinology.* 2009;150:5016–5026.
 34. Castellano JM, Navarro VM, Fernandez-Fernandez R, et al. Changes in hypothalamic KiSS-1 system and restoration of pubertal activation of the reproductive axis by kisspeptin in undernutrition. *Endocrinology.* 2005;146:3917–3925.
 35. Smith JT, Acohido BV, Clifton DK, Steiner RA. KiSS-1 neurones are direct targets for leptin in the *ob/ob* mouse. *J Neuroendocrinol.* 2006;18:298–303.
 36. Donato J Jr, Cravo RM, Frazao R, et al. Leptin's effect on puberty in mice is relayed by the ventral premammillary nucleus and does not require signaling in Kiss1 neurons. *J Clin Invest.* 2011;121:355–368.
 37. Cravo RM, Margatho LO, Osborne-Lawrence S, et al. Characterization of Kiss1 neurons using transgenic mouse models. *Neuroscience.* 2011;173:37–56.
 38. Hill JW, Elias CF, Fukuda M, et al. Direct insulin and leptin action on pro-opiomelanocortin neurons is required for normal glucose homeostasis and fertility. *Cell Metab.* 2010;11:286–297.
 39. Quenell JH, Howell CS, Roa J, Augustine RA, Grattan DR, Anderson GM. Leptin deficiency and diet-induced obesity reduce hypothalamic kisspeptin expression in mice. *Endocrinology.* 2011;152:1541–1550.
 40. Matsuwaki T, Nishihara M, Sato T, Yoda T, Iwakura Y, Chida D. Functional hypothalamic amenorrhea due to increased CRH tone in melanocortin receptor 2-deficient mice. *Endocrinology.* 2010;151:5489–5496.

41. Zigman JM, Jones JE, Lee CE, Saper CB, Elmquist JK. Expression of ghrelin receptor mRNA in the rat and the mouse brain. *J Comp Neurol*. 2006;494:528–548.
42. Hill JW, Xu Y, Preitner F, et al. Phosphatidylinositol 3-kinase signaling in hypothalamic proopiomelanocortin neurons contributes to the regulation of glucose homeostasis. *Endocrinology*. 2009;150:4874–4882.
43. Mesaros A, Koralov SB, Rother E, et al. Activation of Stat3 signaling in AgRP neurons promotes locomotor activity. *Cell Metab*. 2008;7:236–248.
44. Korenbrot CC, Huhtaniemi IT, Weiner RI. Prepubertal separation as an external sign of pubertal development in the male rat. *Biol Reprod*. 1977;17:298–303.
45. Nelson JF, Felicio LS, Randall PK, Sims C, Finch CE. A longitudinal study of estrous cyclicity in aging C57BL/6J mice: I. Cycle frequency, length and vaginal cytology. *Biol Reprod*. 1982;27:327–339.
46. Bingel A, Schwartz NB. Pituitary LH content and reproductive tract changes during the mouse oestrous cycle. *J Reprod Fertil*. 1969;19:215–222.
47. Bruning JC, Michael MD, Winnay JN, et al. A muscle-specific insulin receptor knockout exhibits features of the metabolic syndrome of NIDDM without altering glucose tolerance. *Mol Cell*. 1998;2:559–569.
48. Ohtaki T, Shintani Y, Honda S, et al. Metastasis suppressor gene *KiSS-1* encodes peptide ligand of a G-protein-coupled receptor. *Nature*. 2001;411:613–617.
49. Konner AC, Janoschek R, Plum L, et al. Insulin action in AgRP-expressing neurons is required for suppression of hepatic glucose production. *Cell Metab*. 2007;5:438–449.
50. Safranski TJ, Lamberson WR, Keisler DH. Correlations among three measures of puberty in mice and relationships with estradiol concentration and ovulation. *Biol Reprod*. 1993;48:669–673.
51. Kauffman AS, Clifton DK, Steiner RA. Emerging ideas about kisspeptin-GPR54 signaling in the neuroendocrine regulation of reproduction. *Trends Neurosci*. 2007;30:504–511.
52. Malyala A, Zhang C, Bryant DN, Kelly MJ, Ronnekleiv OK. PI3K signaling effects in hypothalamic neurons mediated by estrogen. *J Comp Neurol*. 2008;506:895–911.
53. Ahmed ML, Ong KK, Dunger DB. Childhood obesity and the timing of puberty. *Trends Endocrinol Metab*. 2009;20:237–242.
54. Jeffery AN, Metcalf BS, Hosking J, Streeter AJ, Voss LD, Wilkin TJ. Age before stage: insulin resistance rises before the onset of puberty: a 9-year longitudinal study (EarlyBird 26). *Diabetes Care*. 2012;35:536–541.
55. Ibanez L, Ong K, Valls C, Marcos MV, Dunger DB, de Zegher F. Metformin treatment to prevent early puberty in girls with precocious pubarche. *J Clin Endocrinol Metab*. 2006;91:2888–2891.
56. Brill DS, Moenter SM. Androgen receptor antagonism and an insulin sensitizer block the advancement of vaginal opening by high-fat diet in mice. *Biol Reprod*. 2009;81:1093–1098.
57. Moret M, Stettler R, Rodieux F, et al. Insulin modulation of luteinizing hormone secretion in normal female volunteers and lean polycystic ovary syndrome patients. *Neuroendocrinology*. 2009;89:131–139.
58. Pesant MH, Dwyer A, Marques Vidal P, et al. The lack of effect of insulin on luteinizing hormone pulsatility in healthy male volunteers provides evidence of a sexual dimorphism in the metabolic regulation of reproductive hormones. *Am J Clin Nutr*. 2012;96:283–288.
59. Navarro VM, Tena-Sempere M. Neuroendocrine control by kisspeptins: role in metabolic regulation of fertility. *Nat Rev Endocrinol*. 2012;8:40–53.
60. Hill JW, Elmquist JK, Elias CF. Hypothalamic pathways linking energy balance and reproduction. *Am J Physiol Endocrinol Metab*. 2008;294:E827–E832.
61. Oakley AE, Clifton DK, Steiner RA. Kisspeptin signaling in the brain. *Endocr Rev*. 2009;30:713–743.
62. Mayer C, Acosta-Martinez M, Dubois SL, et al. Timing and completion of puberty in female mice depend on estrogen receptor α -signaling in kisspeptin neurons. *Proc Natl Acad Sci USA*. 2010;107:22693–22698.
63. Han SK, Gottsch ML, Lee KJ, et al. Activation of gonadotropin-releasing hormone neurons by kisspeptin as a neuroendocrine switch for the onset of puberty. *J Neurosci*. 2005;25:11349–11356.
64. Gottsch ML, Navarro VM, Zhao Z, et al. Regulation of *Kiss1* and dynorphin gene expression in the murine brain by classical and non-classical estrogen receptor pathways. *J Neurosci*. 2009;29:9390–9395.
65. Park CJ, Zhao Z, Glidewell-Kenney C, et al. Genetic rescue of non-classical ER α signaling normalizes energy balance in obese *Era*-null mutant mice. *J Clin Invest*. 2011;121:604–612.
66. Tena-Sempere M. Endocrinology and adolescence: deciphering puberty: novel partners, novel mechanisms. *Eur J Endocrinol*. 2012;167:733–747.
67. Mayer C, Boehm U. Female reproductive maturation in the absence of kisspeptin/GPR54 signaling. *Nat Neurosci*. 2011;14:704–710.
68. Williams KW, Margatho LO, Lee CE, et al. Segregation of acute leptin and insulin effects in distinct populations of arcuate proopiomelanocortin neurons. *J Neurosci*. 2010;30(7):2472–2479.